Bioresources and Bioprocessing

RESEARCH

Enhanced thermal conductivity of waste sawdust-based composite phase change materials with expanded graphite for thermal energy storage

Haiyue Yang[1†], Yazhou Wang[2†], Zhuangchao Liu[3], Daxin Liang[1], Feng Liu[1], Wenbo Zhang[1], Xin Di[1], Chengyu Wang[1*], Shih-Hsin Ho[4*] and Wei-Hsin Chen[5]

Abstract

Background: With the current rapid economic growth, demands for energy are progressively increasing. Energy shortages have attracted significant attention due to the shrinking availability of non-renewable resources. Therefore, thermal energy storage is one of the solutions that lead to saving of fossil fuels and make systems more cost-effective by the storage of wasted thermal energy. In particular, the application of phase change materials (PCMs) is considered as an effective and efficient approach to thermal energy storage because of the high latent heat storage capacity at small temperature intervals. Nevertheless, leakage problems and low thermal conductivity limit the practical applications of PCMs. Therefore, form-stable phase change materials with high thermal conductivity are urgently needed.

Results: A novel form-stable composite phase change material was prepared by incorporating PEG into waste sawdust with 5% EG. In the composites, PEG served as a phase change material, while waste sawdust acted as a carrier matrix. EG was added to help increase the thermal conductivity of the composites. The melting temperature of CPCMs-4 with 5% EG was found to be 58.6 °C with a phase change enthalpy of 145.3 kJ/kg, while the solidifying temperature was 48.5 °C with a phase change enthalpy of 131.4 kJ/kg. The thermal conductivity of CPCMs-4 with 5% EG increased by 23.8% compared with that of CPCMs-4. Moreover, no obvious changes in melting, solidifying temperature, or latent heat after 200 heating–cooling cycles were detected. The supercooling extent of CPCMs-4 with 5% EG decreased by 19.2% compared with PEG. The volume change properties and wettability properties of CPCMs-4 with 5% EG are suitable for thermal energy in terms of practical application.

Conclusions: The prepared composites have excellent thermal and form-stable properties and they can be recognized as potential candidates for thermal energy storage as form-stable composite phase change materials. Using simple impregnation techniques with waste sawdust as a supporting material, this study demonstrates an innovative technology for practically and markedly enhancing the adsorption capacity of phase change materials.

Keywords: Phase change material, Waste sawdust, Second law of thermodynamics, Enhanced thermal conductivity, Wetting properties, Volume expansion percentage

*Correspondence: wangcy@nefu.edu.cn; stephen6949@hit.edu.cn
†Haiyue Yang and Yazhou Wang contributed equally to this study and share first authorship
[1] Key Laboratory of Bio-based Material Science and Technology, Ministry of Education, Northeast Forestry University, Harbin 150040, People's Republic of China
[4] State Key Laboratory of Urban Water Resource and Environment, School of Municipal and Environmental Engineering, Harbin Institute of Technology, Harbin 150090, People's Republic of China
Full list of author information is available at the end of the article

Yang *et al. Bioresour. Bioprocess.* (2017) 4:52

Page 2 of 12

Background

With the current rapid economic growth, demands for energy are progressively increasing. Energy shortages have attracted significant attention due to the shrinking availability of non-renewable resources. Therefore, thermal energy storage, is one of the solutions that leads to saving of fossil fuels and makes systems more cost-effective by the storage of wasted thermal energy (Mateo et al. 2014). In particular, the application of phase change materials (PCMs) is considered as an effective and efficient approach to thermal energy storage because of the high latent heat storage capacity at small temperature intervals (Zeng et al. 2013; Zhang et al. 2013; Tang et al. 2015; Cai et al. 2015). In comparison to inorganic PCMs, organic PCMs can overcome a few of the most fatal deficiencies, including phase separation and super cooling (Qian et al. 2015b). Moreover, organic PCMs also offer some significant advantages, such as good thermal reliability and self-nucleating behavior (Memon 2014). Polyethylene glycol (PEG) has been used widely due to its appropriate phase change temperature and large heat storage capacity (He et al. 2014). In addition, PEG exhibits satisfactory melting behavior, non-toxic and non-corrosive features, excellent chemical and thermal properties, bio-degradability, low vapor pressure, and low cost (Qian et al. 2013). Nevertheless, leakage problems in the melting state still limit the downstream applications of PEG (Qian et al. 2015b).

To solve the problem, some form-stable CPCMs have been fabricated by mixing PEG and supporting materials due to the excellent shape-stabilized properties during the phase transition process (Xu and Li 2014; Chen et al. 2015; Sarı 2015; Lafdi et al. 2008; Tang et al. 2016; Qian et al. 2015a). To achieve the aim of high thermal energy capacity, selecting suitable porous materials with large specific surface areas as the carrier matrices is vital. However, the rising cost of using porous carriers will significantly hinder commercial feasibility. Waste sawdust, a solid waste obtained from furniture manufacturing companies or the papermaking industry, has been widely used in dealing with environmental problems (Luo et al. 2013). Waste sawdust has also been recognized as an absorbent for the removal of dyes, toxic salts, heavy metals, and waste oils from water (Shukla et al. 2002). Because waste sawdust is mainly composed of cellulose (40–50%), lignin (25–40%), and hemicellulose (10–25%) (Li et al. 2014; Collinson and Thielemans 2010), it contains large amounts of hydroxyl, carboxylic, and phenolic groups, which can provide the capacity and structural support needed for PEG. Thus, we demonstrate waste sawdust as a low-cost carrier matrix with great stability for composite phase change materials. Recently, phase change materials interlinked with biomass materials have been

gaining significant attention; however, relevant reports are still rare. For example, Cao et al. (Babapoor et al. 2016) produced shape-stabilized phase change materials based on fatty acid eutectics and cellulose composites. Shin et al. (2015) investigated the thermal property and latent heat energy storage behavior of sodium acetate trihydrate composites containing expanded graphite and carboxymethyl cellulose for phase change materials. However, little is known regarding waste sawdust absorption of phase change materials. In addition, a thorough understanding of the interaction between waste sawdust and phase change materials is still lacking.

In the past few years, a significant number of studies on increasing thermal energy absorbing/releasing speed and improving the heat transfer efficiency of organic PCMs have been conducted (Khodadadi et al. 2013; Fang et al. 2010). Due to the porous structure and enhanced thermal conductivity of expanded graphite (EG), many researchers have employed two or more materials to prepare composite shape-stable phase change materials (e.g., PCMs, EG) (Zhao et al. 2011; Zhong et al. 2010; Sarı and Karaipekli 2007; Zhang et al. 2012; Wang et al. 2014), indicating that efficient enhanced thermal conductivity occurred in composite shape-stable phase change materials. Some reports have suggested that EG has great application potentials in the field of phase change materials (Huang et al. 2014; Tian et al. 2015).

In this study, properties of novel PEG/waste sawdust composites with enhanced thermal conductivity for thermal energy storage were investigated. In the composites, PEG served as a phase change material while waste sawdust acted as a carrier matrix. To the best of our knowledge, waste sawdust used as supporting materials are firstly introduced into the phase change materials. In addition, because of its superior performance, EG was added to help increase the thermal conductivity of the composites. On the basis of the thermal conductivity meter (TCM), the thermal conductivity of the optimal sample increased by 23.8% compared to when there was no expanded graphite in the composites with a mass ratio of PEG to waste sawdust of 4:1. All the results of this study indicated that a waste sawdust-based form-stable CPCMs could be a potential candidate for efficient thermal energy storage.

Methods

Materials

Analytical reagent PEG with an average molecular weight of 10,000 was offered by Tianjin Tianli Chemical Co., Ltd. (Tianjin, China). Absolute ethanol (Analytical reagent) was obtained from Tianjin Chemical Reagent Co., Ltd (Tianjin, China). Expanded graphite was purchased from the Qingdao Graphite Co. Ltd (Qingdao, China). Waste

Yang *et al. Bioresour. Bioprocess.* (2017) 4:52

Page 3 of 12

sawdust (poplar, grain diameter of 178–250 μm) was a lab-made material derived in Carpenter's laboratory at Northeast Forestry University (Heilongjiang province, China).

Preparation of the composite phase change materials

The composite phase change materials (CPCMs) were obtained by mixing the waste sawdust, PEG, and EG with a weight ratio of 4:16:1. Firstly, waste sawdust was ultrasonically cleaned with absolute ethanol and deionized water for 10 min, respectively. Then it was dried at 60 °C for 12 h in an oven. After that, waste sawdust, PEG, and EG were each dispersed into absolute ethanol with quick stirring for 3 h at 25 °C, respectively. And then, the above three kinds of ethanol mixture were mixed again under stirring for 1 h at 25 °C. Finally the samples kept static at 110 °C in a vacuum oven for 12 h until the absolute ethanol was evaporated completely. The composite phase change materials were thus obtained. The synthetic route for the PEG/waste sawdust with EG composites is shown in Fig. 1.

In order to study the optimal mass fraction of PEG in the composites, a range of the PEG/waste sawdust mixtures were determined (mass fractions of PEG: 20, 40, 60, 80, 81, 82, 83, 84, and 85%). The liquid leakage test method was carried out as follows: different samples with various mass fractions of PEG were put on pieces of weigh paper, which have been weighed and numbered, respectively. Each sample kept static at 70 °C for 30 min before at 80 °C for 30 min in an oven. Then, each piece of weigh paper was weighed again. Compared with first weight, it can be determined whether there is a leakage happening in the processing of phase change. The optimal mass fraction of PEG in the composites was found to be 80%. Four samples were obtained, which were labeled as CPCMs-1, CPCMs-2, CPCMs-3, and CPCMs-4, individually. CPCMs-4 with 1% EG, CPCMs-4 with 3% EG, and CPCMs-4 with 5% EG were also obtained, respectively. The mass fractions of the PEG, waste sawdust, and EG in these samples are presented in Table 1.

Characterization analysis

A Fourier transformation infrared spectroscope (FTIR, Thermo Fisher Scientific Nicolet 6700, USA) was employed to estimate the chemical structure from 400 to 4000 cm^{-1} with a resolution of 4 cm^{-1}. The crystal structure was analyzed with an X-ray diffractometer (XRD, D/max 2200VPC, Rigaku, Japan) from 5° to 50° at room temperature. The surface microstructure of samples were observed with a scanning electron microscopy (SEM, Hitachi TM3030). The thermal properties of CPCMs are measured with a differential scanning calorimeter (DSC, Q20, TA, USA) from 25 to 100 °C at 5 °C/min under nitrogen at a flow rate of 20 mL/min. Thermogravimetric analysis (TGA) was carried out on a STA

Table 1 The conditions of different composite phase change materials

Samples	PEG (%)	Waste sawdust (%)	EG (%)
CPCMs-1	20	80	–
CPCMs-2	40	60	–
CPCMs-3	60	40	–
CPCMs-4	80	20	–
CPCMs-4 + 1% EG	80	20	1
CPCMs-4 + 3% EG	80	20	3
CPCMs-4 + 5% EG	80	20	5
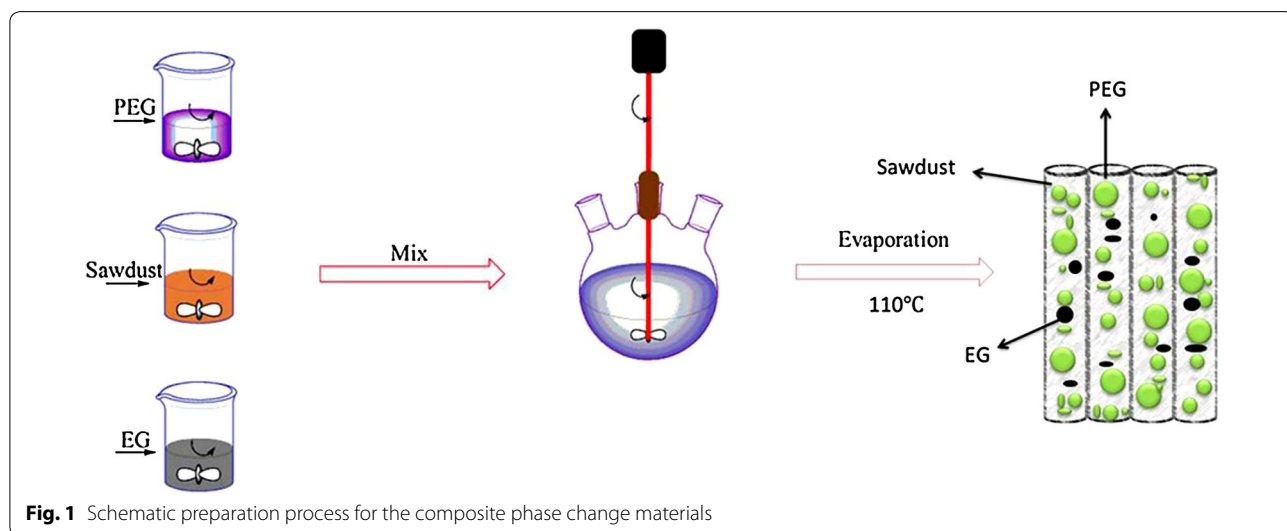
Fig. 1 Schematic preparation process for the composite phase change materials

Yang *et al. Bioresour. Bioprocess.* (2017) 4:52

Page 4 of 12

6000-SQ8 thermal analyzer (0.1 mg, ± 1 °C) with heating rate of 10 °C/min under nitrogen atmosphere. The thermal conductivity of CPCMs was obtained by a thermal conductivity meter (TCM, TPS 2500s, Hot Disk, Sweden). The contact angle was collected using a video-based contact angle measuring device (OCA 20, Dataphysics, Germany).

Results and discussion

FTIR analysis

An FTIR analysis was used to estimate the chemical structures of the PEG, waste sawdust, and EG. The FTIR spectrums of (a) PEG, (b) CPCMs-4, (c) CPCMs-4 with 5% EG, and (d) waste sawdust are displayed in Fig. 2. In Fig. 2a, the two typical peaks of PEG were respectively 962 and 2906 cm^{-1}. The peak at 962 cm^{-1} is the stretching vibrations of C–H, and the peak at 2906 cm^{-1} belongs to –CH$_2$ stretching vibrations of PEG (Qian et al. 2015b). At wave numbers of 1109 and 3403 cm^{-1}, the stretching vibration peaks of C–O and –OH were discovered, respectively. Figure 2d is a typical spectrum of waste sawdust. Due to the existence of hydrogen and oxygen compounds in wood, such as cellulose, hemicellulose, and lignin, the peaks at around 3329 and 2280 cm^{-1} are, respectively, the stretching vibrations of –OH and –CH$_2$ in the waste sawdust. Figure 2c shows the characteristic absorption peaks at a wavenumber of 1636 cm^{-1}, corresponding to the stretching vibrations of C=O. In Fig. 2b, c, the stretching vibration peaks of –OH disappeared, suggesting that it may form a hydrogen bond caused by the –OH of PEG and the waste sawdust. Apart from some mild peak slips (e.g., –CH$_2$–OH), the main PEG and waste sawdust peaks appeared as expected. The results indicated that no significant new peaks were discovered, indi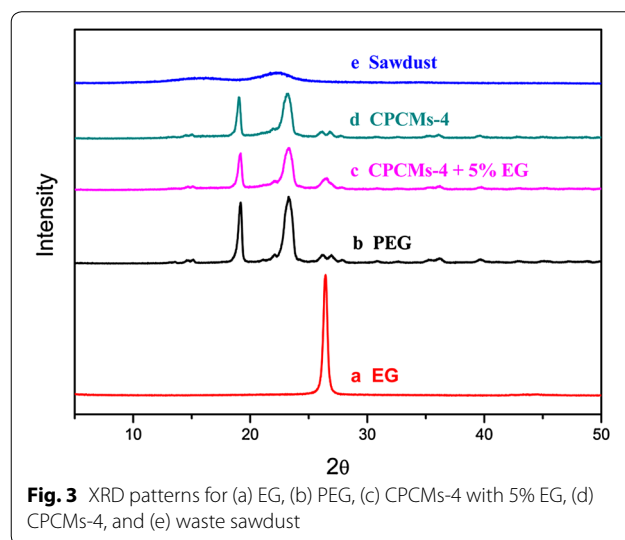cating that there are no chemical interactions between PEG and waste sawdust, which is beneficial in terms of the form stability of the composites.
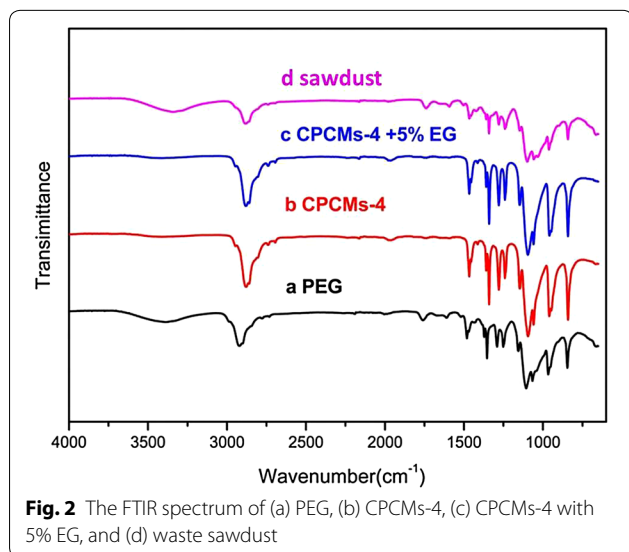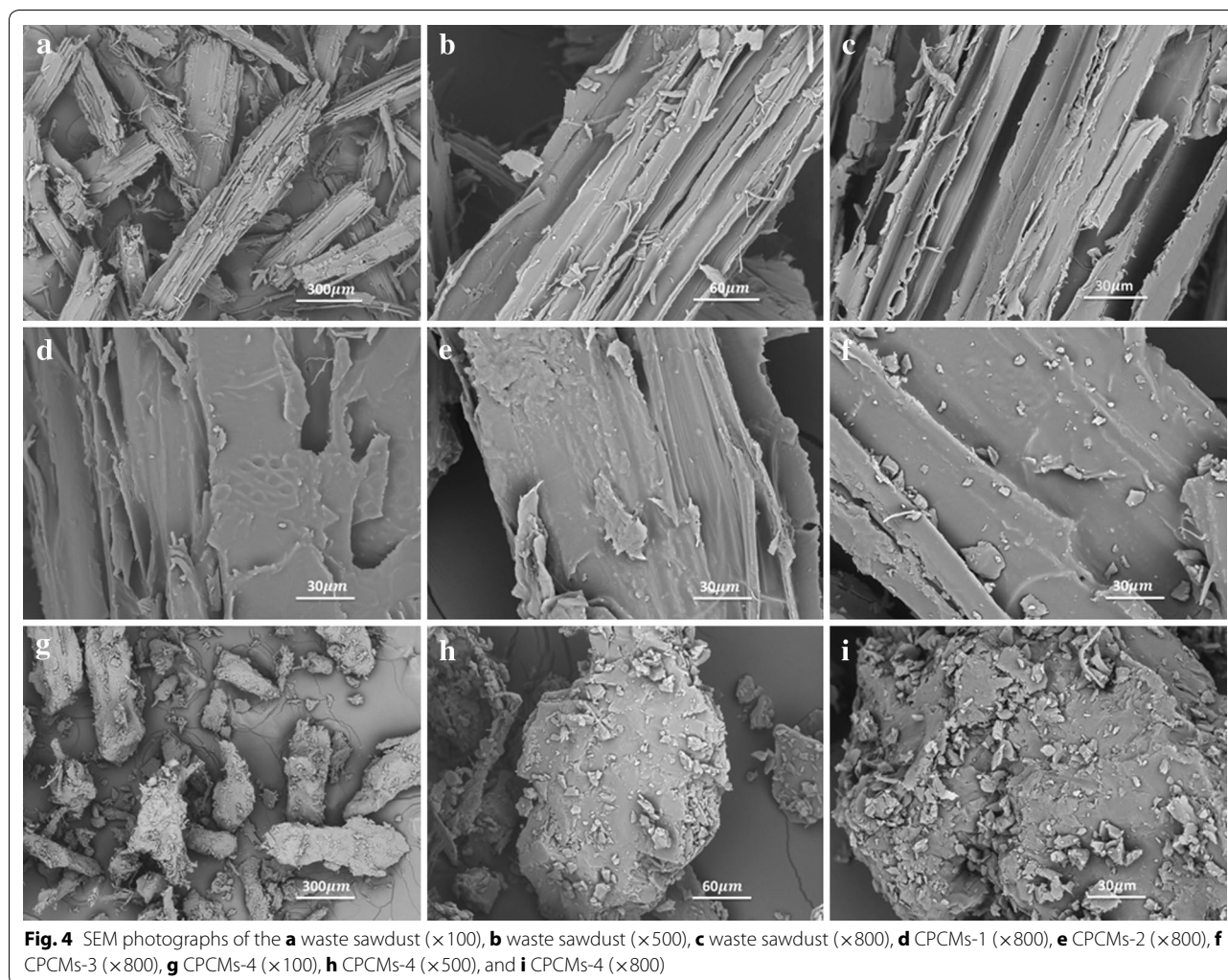
XRD analysis of the form-stable CPCMs

XRD was employed to investigate crystalline properties of the composites. Figure 3 displays the XRD patterns of (a) EG, (b) PEG, (c) CPCMs-4 with 5% EG, (d) CPCMs-4, and (e) waste sawdust. As shown in Fig. 3a, the steep peak at 26.5° was attributed to the crystal structure of EG. Two distinct steep peaks at about 19.3° and 23.2° were allocated to PEG crystal (Fig. 3b) while 22.2° was assigned to waste sawdust (curve e). Figure 3d displays the characteristic diffraction peaks of PEG and waste sawdust. In addition, in Fig. 3c, the PEG, waste sawdust, and EG-specific diffraction peaks appeared simultaneously, and no obvious peak changes were observed. These results suggest that the crystalline structures of the PEG, waste sawdust, and EG were not destroyed by the formation of the composite phase change material composed of PEG/waste sawdust and EG, which further suggests that no significant mutual effect occurred between the PEG, waste sawdust, and the EG.

Microstructure of the form-stable CPCMs

Figure 4 shows scanning electron microscope photographs of waste sawdust and CPCMs-1-4. Figure 5 presents the SEM photography of CPCMs-4 with EG. Figure 4c distinctly shows the microstructure of the waste sawdust. It reveals that a tubular structure emerged in the waste sawdust, along with numerous pores on the tube. Compared with Fig. 4c, d, f, shows that the PEG was absorbed into the pores and tubes, indicating that it was uniformly absorbed into the waste sawdust structure. In Fig. 4i, in addition, it can be seen that the waste sawdust

Fig. 2 The FTIR spectrum of (a) PEG, (b) CPCMs-4, (c) CPCMs-4 with 5% EG, and (d) waste sawdust

Fig. 3 XRD patterns for (a) EG, (b) PEG, (c) CPCMs-4 with 5% EG, (d) CPCMs-4, and (e) waste sawdust

Yang *et al. Bioresour. Bioprocess.* (2017) 4:52

Page 5 of 12

Fig. 4 SEM photographs of the **a** waste sawdust (×100), **b** waste sawdust (×500), **c** waste sawdust (×800), **d** CPCMs-1 (×800), **e** CPCMs-2 (×800), **f** CPCMs-3 (×800), **g** CPCMs-4 (×100), **h** CPCMs-4 (×500), and **i** CPCMs-4 (×800)

pores had absorbed much more PEG and that the tube structure and microstructure pores in the waste sawdust had disappeared. However, a comparison of Fig. 4g, h with Fig. 4a, b indicates no obvious changes in the fundamental shape, suggesting that the composites may remain form-stable during the phase change process.

Figure 5 displays the SEM images of CPCMs-4 with 1% EG, CPCMs-4 with 3% EG, and CPCMs-4 with 5% EG, demonstrating that EG disperses uniformly into CPCMs-4, which is in a good agreement with a previous study indicating that the addition of EG can help improve the thermal conductivity of PCMs and prevent liquids from leaking in composite phase change materials. Therefore, in this study, a novel form-stable composite phase change material with enhanced thermal conductivity was obtained.

Wetting properties of a composite phase change material
The absorption theory suggested that wettability properties of solid materials are especially significant in many

fields (Wang et al. 2017). A low contact angle (< 90°) shows that the solid material is wettable. And the liquid will be absorbed into solid materials. The contact angle is the angle at which a liquid/vapor interface meets the solid surface. And it is determined by the interactions across the three interfaces (Fig. 6) (Zhenyu et al. 2016).

$$\cos\theta = (\gamma_{SV} - \gamma_{SL})/\gamma_{LV}, \tag{1}$$

where the parameters of γ_{SV}, γ_{SL}, and γ_{LV} are respectively the solid–vapor, solid–liquid, and liquid–vapor interfacial tensions, and where θ is the contact angle. In order to estimate the absorption performance indirectly, the wetting properties of different supporting materials were measured in this study. An ethanol solution of PEG could be quickly absorbed into waste sawdust within 2 s and the contact angle approaches 0°, which shows that waste sawdust has good wettability. The dynamic absorption process is shown in the Additional file 1: Video S1. Table 2 displays the maximum
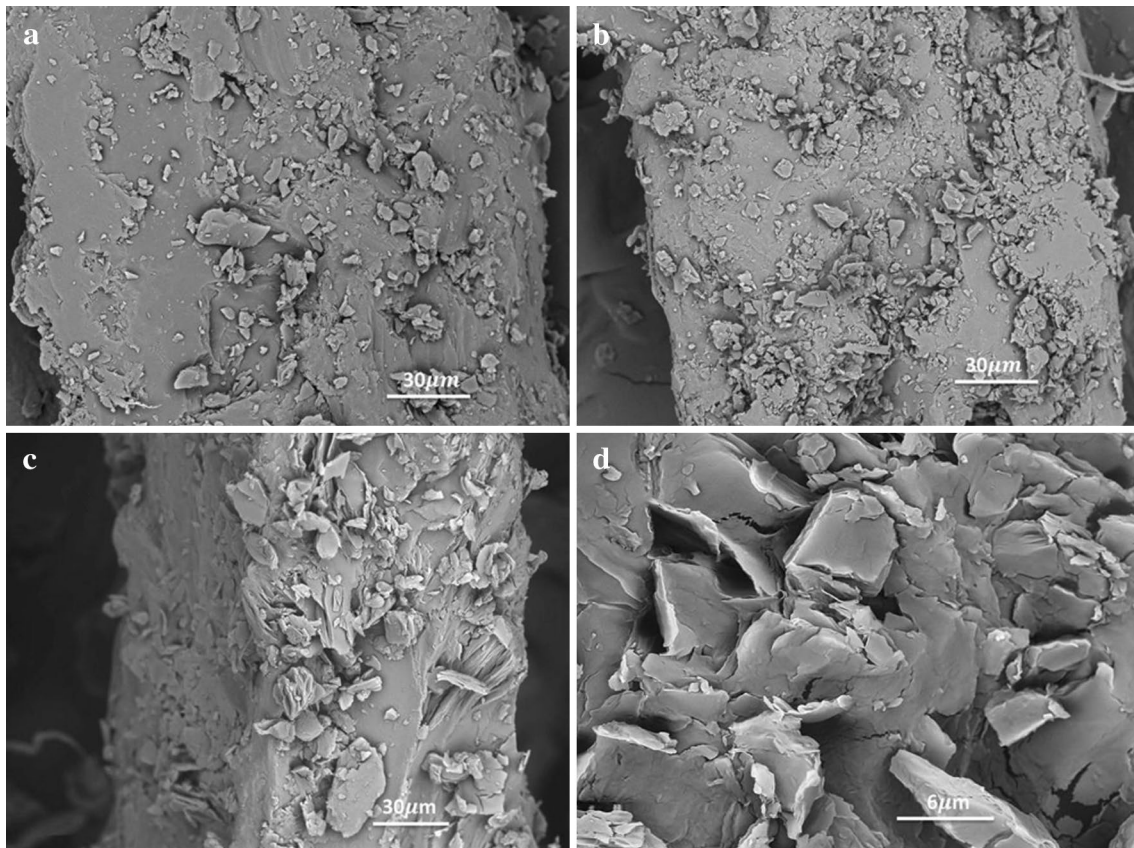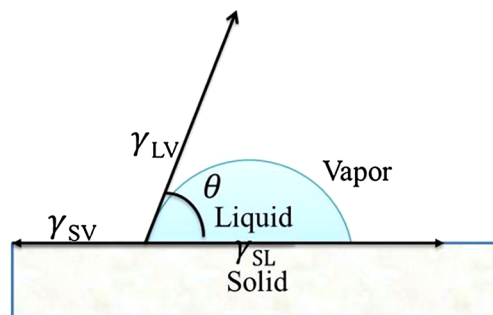
Yang *et al. Bioresour. Bioprocess.* (2017) 4:52

Page 6 of 12

Fig. 5 SEM photographs of the **a** CPCMs-4 with 1% EG (×800), **b** CPCMs-4 with 3% EG (×800), **c** CPCMs-4 with 5% EG (×800), and **d** CPCMs-4 with 5% EG (×5.0k)

Schematic diagram of contact angle of waste sawdust -ethanol solution of PEG-vapor system

Fig. 6 A schematic diagram of the solid–liquid–vapor system contact angle

Table 2 Mass fraction of PEG and time required for the ethanol solution with PEG to diffuse into the supporting materials

Supporting material	Maximum mass fraction of PEG (wt%)	Time required for the ethanol solution with PEG to diffuse into the supporting material(s)
Hydroxyapatite	70 (Wang et al. 2017)	7
Calcium silicate	70 (Qian et al. 2015b)	10
Active carbon	70 (Feng et al. 2011)	11
Sawdust	80	2

Yang *et al. Bioresour. Bioprocess.* (2017) 4:52

Page 7 of 12

mass fraction of PEG in the supporting materials and the time required for the ethanol solution with PEG to diffuse into the supporting materials. The time required for diffusing into waste sawdust was 2 s, which is much lower than that of hydroxyapatite (7 s), calcium silicate (10 s), active carbon (11 s), but the maximum mass fraction of PEG is larger than that of hydroxyapatite (70%), calcium silicate (70%), and active carbon (70%), indicating that waste sawdust has excellent wetting property as compared to hydroxyapatite, calcium silicate, and active carbon. The results confirm that waste sawdust has good wettability and that waste sawdust can be a potential supporting material for absorbing phase change materials.

Form-stable property

A drying oven was used to characterize the shape-stable properties of PEG (Fig. 7a), CPCMs-4 (Fig. 7b), and CPCMs-4 with 5% EG (Fig. 7c). Every given temperature was held for 30 min, and a digital camera was employed to record the results. As depicted in Fig. 7, at a temperature of 70 °C, the PEG melted quickly. On the contrary, the structures of both CPCMs-4 and CPCMs-4 with 5% EG remained constant. With an increase in the temperature to 80 °C, the PEG melted completely into liquid while CPCMs-4 and CPCMs-4 with 5% EG remained solid due to the presence of waste sawdust, which provided dramatic support to the composite structure. No liquid leakage was found on the CPCMs-4 and CPCMs-4 with 5% EG weigh paper, thus demonstrating that the masses and structure of the CPCMs-4 and CPCMs-4 samples with 5% EG remained constant both before and after the thermal test.

The results clearly indicate that the prepared composite phase change material was shape stable without any liquid leakage from the supporting materials, which infers a significant contribution to the field of thermal energy storage. In addition, in regard to the test of the CPCMs-4 heating–cooling cycles, Fig. 8 shows that there were no obvious changes in the melting and solidifying temperatures before and after 200 and 1000 heating–cooling cycles (denoted as CPCMs-4c, CPCMs-4c$_1$ after 200 and 1000 heating–cooling cycles, respectively). The melting temperature of CPCMs-4 before and after the 200 and 1000 heating–cooling cycles was, respectively, 58.1, 59.5, and 58.9 °C, while the solidifying temperatures of CPCMs-4 before and after the cycles were, respectively, 48.6, 48.7, and 48.4 °C. In addition, the latent heat required for melting for CPCMs-4 before and after the cycles was, respectively, 151.1, 143.0, and 126.4 kJ/kg. The latent heat required for solidifying of CPCMs-4 before and after the cycles was, respectively, 140.3, 133.7, and 117.5 kJ/kg. After the cycles, the melting enthalpy decreased by 5.4 and 16.4%, respectively, and the solidifying enthalpy decreased by 4.7 and 16.2%, respectively. This indicated that no obvious changes were found in terms of latent heat and phase change temperatures, thus verifying that CPCMs-4 has good thermal reliability.

Thermal properties of the composite phase change materials

The phase change latent and the temperature of CPCMs were obtained by a differential scanning calorimeter (DSC). The melting and solidifying DSC curves of (a) PEG, (b) CPCMs-1, (c) CPCMs-2, (d) CPCMs-3, and (e) CPCMs-4 are illustrated in Fig. 9. In addition, the melting and solidifying curves of (a) PEG, (b) CPCMs-4 with 5% EG, and (c) CPCMs-4 are depicted in Fig. 10. The thermal data of the CPCMs are shown in Table 3.
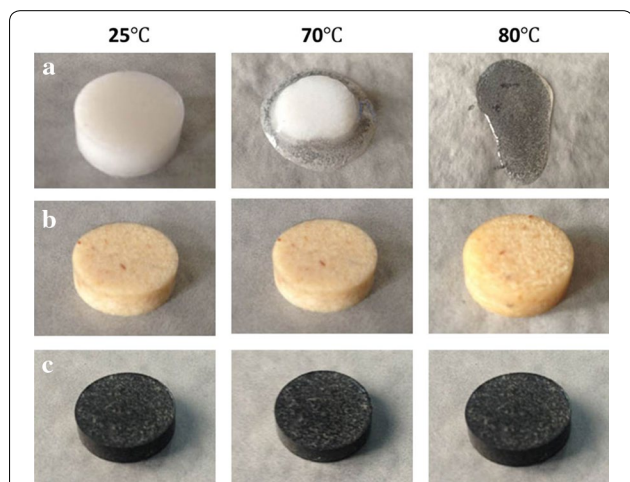

Fig. 7 Shape-stable images of **a** PEG, **b** CPCMs-4, and **c** CPCMs-4 with 5% EG
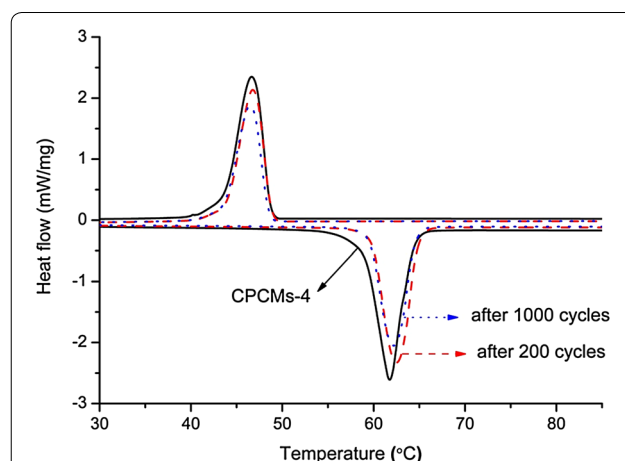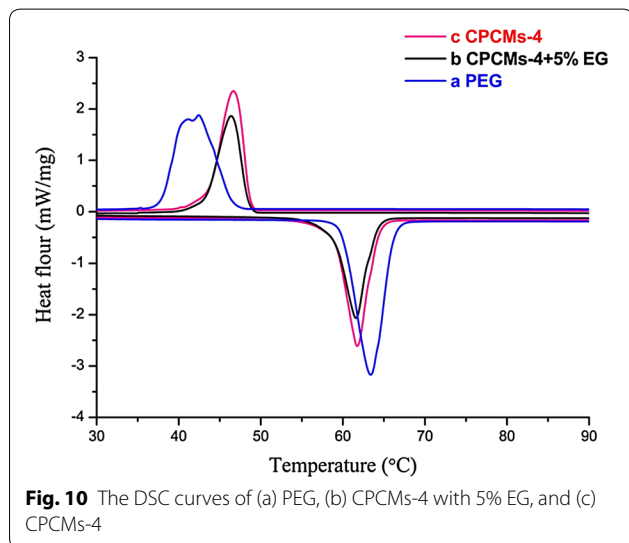

Fig. 8 The DSC curves of CPCMs-4 before and after experiencing either 200 or 1000 heating–cooling cycles

Yang *et al. Bioresour. Bioprocess.* (2017) 4:52

Page 8 of 12

Fig. 9 The DSC curves of (a) PEG, (b) CPCMs-1, (c) CPCMs-2, (d) CPCMs-3, and (e) CPCMs-4

Fig. 10 The DSC curves of (a) PEG, (b) CPCMs-4 with 5% EG, and (c) CPCMs-4
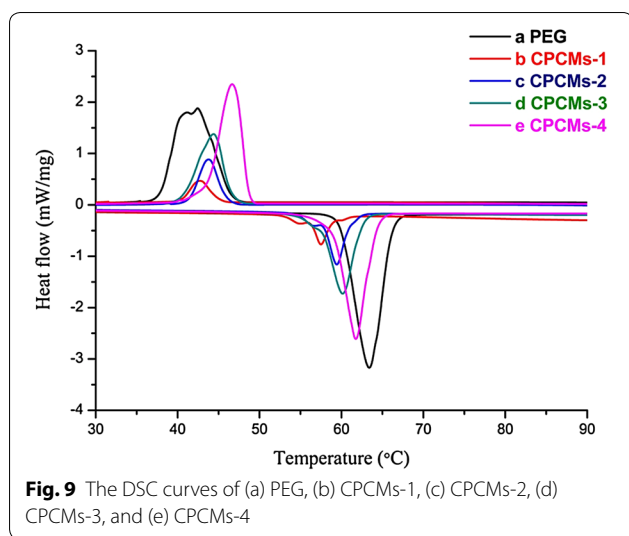
The phase change latent is regarded as one of the most critical factors to assess the thermal energy storage capacity of CPCMs. As a matter of fact, the thermal energy capacity of CPCMs rests with the PEG content in the composites. A higher PEG content will significantly improve the phase change latent; however, the higher PEG content will also increase the possibility of liquid leakage. Taken together, both PEG content and form-stable properties are recognized as two critical factors, which can influence thermal energy storage capacity of CPCMs. In this study, the maximum mass fraction of PEG in the CPCMs was 80% without any liquid leakage during the phase transition (Fig. 7b). As shown in Table 3, the melting temperatures of PEG and CPCMs-1-4 were, respectively, 59.0, 56.8, 57.2, 57.3, and 58.1 °C while the melting enthalpy is 189.5, 37.8, 76.0, 111.2, and 151.1 kJ/kg. The solidifying temperatures of PEG and CPCMs-1-4 were, respectively, 46.5, 44.9, 45.9, 46.4, and 48.6 °C while the solidifying enthalpy is 172.5, 29.1, 69.9, 105.3, 140.3 kJ/kg. The melting temperatures of CPCMs-4 with 1% EG, CPCMs-4 with 3% EG, and CPCMs-4 with 5% EG were, respectively, 58.1, 58.0, and 58.6 °C. The solidifying temperatures were, respectively, 48.3, 48.0, and 48.5 °C. These results demonstrate that the phase change properties of CPCMs-4 with EG are very similar to those of the PEG mixture, suggesting that waste sawdust, EG, and PEG are compatible. The melting phase change enthalpies of CPCMs-4, CPCMs-4 with 1% EG, CPCMs-4 with 3% EG, and CPCMs-4 with 5% EG were, respectively, 151.1, 150.1, 148.6, and 145.3 kJ/kg, while their solidifying phase change enthalpies were 140.3, 138.3, 135.2, and 131.4 kJ/kg, respectively. Due to the low content of EG (i.e., 1–5%), the phase change enthalpy of the composites did not significantly decline, indicating that the heat storage capacity did not change significantly with a low mass fraction of EG. In composite phase change materials, the

Table 3 Thermal characteristics of CPCMs-1, CPCMs-2, CPCMs-3, CPCMs-4, CPCMs-4c, CPCMs-4c$_1$, CPCMs-4 with 1% EG, CPCMs-4 with 3% EG, CPCMs-4 with 5% EG and PEG

Samples	Mass fraction of PEG (wt%)	T_m (°C)	T_s (°C)	ΔH_m (kJ/kg)	ΔH_s (kJ/kg)
CPCMs-1	20.0	56.8 ± 0.1	44.9 ± 0.3	37.8 ± 1.7	29.1 ± 2.1
CPCMs-2	40.0	57.2 ± 0.1	45.9 ± 0.2	76.0 ± 2.4	69.9 ± 3.0
CPCMs-3	60.0	57.3 ± 0.1	46.4 ± 0.1	111.2 ± 2.4	105.3 ± 1.4
CPCMs-4	80.0	58.1 ± 0.1	48.6 ± 0.1	151.1 ± 1.8	140.3 ± 2.6
CPCMs-4c	–	59.5 ± 0.1	48.7 ± 0.2	143.0 ± 2.3	133.7 ± 2.7
CPCMs-4c$_1$	–	58.9 ± 0.1	48.4 ± 0.2	126.4 ± 2.5	117.5 ± 1.9
CPCMs-4 + 1% EG	79.2	58.1 ± 0.2	48.3 ± 0.1	150.1 ± 3.6	138.3 ± 2.0
CPCMs-4 + 3% EG	77.7	58.0 ± 0.3	48.0 ± 0.2	148.6 ± 2.4	135.2 ± 3.7
CPCMs-4 + 5% EG	76.2	58.6 ± 0.2	48.5 ± 0.2	145.3 ± 2.6	131.4 ± 2.5
PEG	100	59.0 ± 0.4	46.5 ± 0.2	189.5 ± 1.4	172.5 ± 1.9

Yang *et al. Bioresour. Bioprocess.* (2017) 4:52

Page 9 of 12

phase change process comes from PEG, the phase change enthalpy of CPCMs can be obtained by the Eq. (2):

$$\Delta H_{CPCMs} = \Delta H_{PCM} \times \eta, \tag{2}$$

where the parameter of η is the mass fraction of PEG in the composites, and ΔH_{PCM} is the phase change enthalpy of the PCMs.

From CPCMs-1 to CPCMs-4, it displays that, with the increase of PEG, phase change temperatures rise. The reason would be explained by the second law of thermodynamics applying in the phase change process.

$$T = \frac{\Delta H}{\Delta S}, \tag{3}$$

where T is the phase change temperature of CPCMs, ΔH the phase change heat per unit mass, and ΔS is the entropy change during phase change transition. With the increasing mass fraction of PEG, ΔH improves while ΔS decreases. Therefore, the phase change temperature decreases. Compared with CPCMs-1-3, entropy change is the least and phase change enthalpy is the largest. That is the reason why DSC curves of CPCMs-4 is significantly different from CPCMs-1-3. According to the entropy formula, the entropy will be larger with mass fraction of PEG. Compared with PEG, waste sawdust has larger expansion ratio because of porous structure during the phase change transition. In consequence, the phase change temperature of CPCMs will become larger.

Supercooling as another important parameter in practical applications that should be taken into consideration. Lowering the extent of supercooling can assist the phase change transition process. In accordance with Table 3, the degree of supercooling can be obtained as the difference between the melting and solidifying temperature. Figure 11 shows the extent of supercooling for
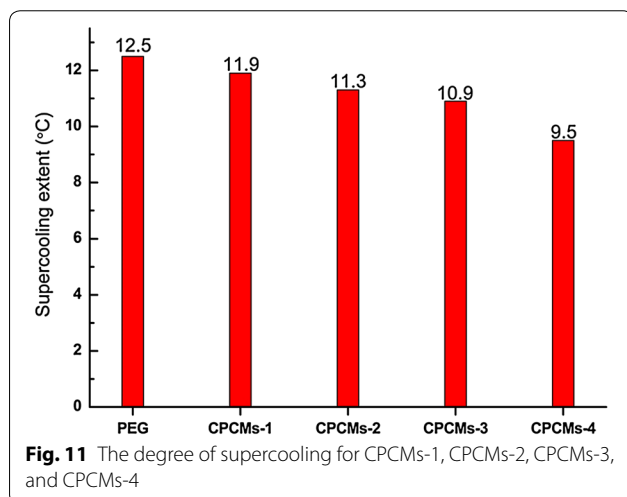

Fig. 11 The degree of supercooling for CPCMs-1, CPCMs-2, CPCMs-3, and CPCMs-4

PEG, CPCMs-1, CPCMs-2, CPCMs-3, and CPCMs-4. Compared with PEG, the degree of supercooling of the CPCMs gradually decreased with the increasing mass fraction of PEG. The degree of supercooling of CPCMs-1, CPCMs-2, CPCMs-3, CPCMs-4, CPCMs-4 with 1% EG, CPCMs-4 with 3% EG, and CPCMs-4 with 5% EG were, respectively, reduced by 4.8, 9.6, 12.8, 24.0, 21.6, 20.0, and 19.2% compared with the PEG. The results show that the degree of supercooling for the optimal sample can effectively reduce to 24.0% by adding 20% waste sawdust.

Volume change during the phase change transition process

Thermal expansion is the tendency of change in shape, area, and volume due to the change of temperature. The volume change of PCMs occur during the phase change transition process. Theoretically, a lower volume change of CPCMs is more suitable for thermal energy storage in practical applications because a large expansion percentage can cause damage to the surrounding environment, such as corrosion, volume deformation, and so on. In this study, the volume expansion ratio is defined as the following Eq. (4):

$$\gamma_V = (V_1 - V_0) / V_0, \tag{4}$$

where the parameters V_0 and V_1 are the volumes of the prepared sample at room temperature and at 70 °C maintained for 30 min, respectively. 0.6 g of waste sawdust, CPCMs-1, CPCMs-2, CPCMs-3, and CPCMs-4 and PEG were accurately weighed. Then, the samples were pressed into cylinders (the diameter was 13 mm) under a pressure of 15 Mpa. Table 4 shows the height, diameter, and volume ($V_0 = 0.25 \times \pi \times D_0^2 \times H_0$, $V_1 = 0.25 \times \pi \times D_1^2 \times H_1$) changes for the samples. The volume expansion ratios of waste sawdust, CPCMs-1, CPCMs-2, CPCMs-3, CPCMs-4, and PEG were, respectively, 6.50, 22.02, 23.59, 15.86, 14.22, and 25.64%. These results indicate that the volume expansion ratio of CPCMs-4 is much lower than that of PEG, which shows that CPCMs-4 have good thermal dimensional stability and it is promising for thermal energy storage in practical application.

Thermal conductivity of the form-stable composite phase change material

The thermal conductivity was estimated with a thermal conductivity meter (TCM) at the test temperature of 24 °C. As shown in Table 5, the thermal conductivity of CPCMs-4, CPCMs-4 with 1% EG, CPCMs-4 with 3% EG, and CPCMs-4 with 5% EG was, respectively, 0.1156 W/(m K), 0.1202 W/(m K), 0.1371 W/(m K), and

Yang *et al. Bioresour. Bioprocess.* (2017) 4:52

Page 10 of 12

Table 4 The height, diameter, and volume change of tablet samples

Sample	D_0 (mm)	D_1 (mm)	H_0 (mm)	H_1 (mm)	V_0 (mm^3)	V_1 (mm^3)	(%)
CPCMs-1	13.00	13.12	3.94	4.72	522.70	637.79	22.02 ± 0.27
CPCMs-2	13.00	13.14	3.72	4.50	493.51	609.92	23.59 ± 0.26
CPCMs-3	13.00	13.08	3.60	4.12	469.63	553.33	15.86 ± 0.27
CPCMs-4	13.00	13.34	3.54	3.84	469.63	536.43	14.22 ± 0.30
PEG	13.00	–	3.6	–	477.60	600.02	25.64 ± 0.49

Table 5 Thermal conductivity of CPCMs-4, CPCMs-4 with 1% EG, CPCMs-4 with 3% EG, and CPCMs-4 with 5% EG

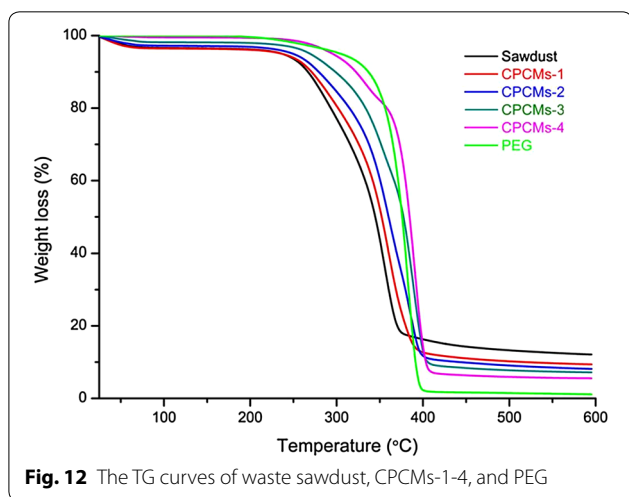| Samples	Thermal conductivity (W/(m))
CPCMs-4	0.1156 ± 0.0016
CPCMs-4 + 1%	0.1202 ± 0.0022
CPCMs-4 + 3%	0.1371 ± 0.0029
CPCMs-4 + 5%	0.1431 ± 0.0011

Fig. 12 The TG curves of waste sawdust, CPCMs-1-4, and PEG

0.1431 W/(m K). Compared with CPCMs-4, the thermal conductivity of CPCMs-4 increased with an increase in EG content, which is in a good agreement with the findings of a previous study (Tang et al. 2015). The greatest enhancement of 23.8% was obtained in CPCMs-4 with 5% EG, clearly indicating that adding small amounts of EG into the composites could significantly enhance the thermal conductivity. The increase in thermal conductivity is more likely due to the thermal conductive network formed by EG (Sobolciak et al. 2016).

Thermal stability

The thermal stability of the pure components (PEG and waste sawdust) and prepared composites (CPCMs-1-4) was evaluated using the TGA analysis, as shown in Fig. 12. In the waste sawdust curves, about 3% weight loss in the absorbed water, including the bound water and a small amount of free water, was observed. With increases in the mass fraction of PEG, the amount of absorbed water declined. The CPCMs-4 curve did not exhibit any absorbed water. Rapid weight loss for the waste sawdust, CPCMs-1-4, and PEG occurred at 356.1, 361.5, 384.4, 388.3, 389.6, and 383.0 °C, respectively. CPCMs were thermally stable when temperatures were below 150 °C. As a result, the CPCMs obtained in this study were quite stable at their working temperatures, which ensured their feasibility for practical application. The results clearly indicate that adding PEG into waste sawdust not only can improve the thermal stability of waste sawdust but can also enhance the humidity resistance of the waste sawdust, so its use can be applied in the real world.

Conclusions

In this study, a novel form-stable composite phase change material was prepared and comprehensively characterized. The melting temperature of CPCMs-4 with 5% EG was found to be 58.6 °C with a phase change enthalpy of 145.3 kJ/kg, while the solidifying temperature was 48.5 °C with a phase change enthalpy of 131.4 kJ/kg. The thermal conductivity of CPCMs-4 with 5% EG increased by 23.8% compared with that of CPCMs-4. Moreover, no obvious changes in melting, solidifying temperature, or latent heat after 200 heating–cooling cycles were detected. The supercooling extent of CPCMs-4 with 5% EG decreased by 19.2% compared with PEG. The volume change properties and wettability properties of CPCMs-4 with 5% EG are suitable for thermal energy in terms of practical application. All these results strongly suggest that the prepared composites have excellent thermal and form-stable properties and that they can be recognized as

Yang *et al. Bioresour. Bioprocess.* (2017) 4:52

Page 11 of 12

potential candidates for thermal energy storage as form-stable composite phase change materials. Using simple impregnation techniques with waste sawdust as a supporting material, this study demonstrates an innovative technology for practically and markedly enhancing the adsorption capacity of phase change materials. The superior performance and novel characterization methods were also discussed in detail.

In the future, different bio-based materials will be applied to the field of CPCMs due to their non-toxicity, recyclability, low cost, and environmental friendliness. And different properties of CPCMs, for example, fire retardation and intelligent response performance, will be studied in the future study trend.

Additional file

> **Additional file 1: Video S1.** The dynamic adsorption process of waste sawdust.

Abbreviations
PEG: polyethylene glycol; EG: expanded graphite; CPCMs: composite phase change materials; TCM: thermal conductivity meter; FTIR: Fourier transformation infrared spectroscope; XRD: X-ray diffractometer; DSC: differential scanning calorimeter; CPCMs-1: 80% PEG + 20% waste sawdust composite phase change materials; CPCMs-2: 60% PEG + 40% waste sawdust composite phase change materials; CPCMs-3: 40% PEG + 60% waste sawdust composite phase change materials; CPCMs-4: 20% PEG + 80% waste sawdust composite phase change materials; SEM: scanning electron microscope; γ_{SV}, γ_{SL}, and γ_{LV}: the solid–vapor, solid–liquid, and liquid–vapor interfacial tensions, respectively; θ: contact angle; CPCMs-4c: after 200 heating–cooling cycles; CPCMs-4c$_1$: after 1000 heating–cooling cycles; η: the mass fraction of PEG in the composites; ΔH_{PCM}: the phase change enthalpy of the PCMs; T: phase change temperature of CPCMs; ΔH: the phase change heat per unit mass; ΔS: the entropy change during phase change transition.

Authors' contributions
HY and YW designed the study, performed experiments, analyzed data, and prepared the manuscript. ZL, DL, FL, WZ, and XD contributed to the discussion. CY, SHH, and WHC reviewed the results, helped in data analysis, and edited the manuscript. All authors read and approved the final manuscript.

Author details
[1] Key Laboratory of Bio-based Material Science and Technology, Ministry of Education, Northeast Forestry University, Harbin 150040, People's Republic of China. [2] School of Material Science and Engineering, Sun Yat-Sen University, Guangzhou 510275, People's Republic of China. [3] Guangdong Yihua Timber Industry Co., Ltd, Guangzhou 510000, People's Republic of China. [4] State Key Laboratory of Urban Water Resource and Environment, School of Municipal and Environmental Engineering, Harbin Institute of Technology, Harbin 150090, People's Republic of China. [5] Department of Aeronautics and Astronautics, National Cheng Kung University, Tainan 701, Taiwan.

Competing interests
The authors declare that they have no competing interests.

Availability of data and materials
The dataset (graphs and tables) supporting the conclusions of this article is available.

Consent for publication
Not applicable.

Ethics approval and consent to participate
Not applicable.

Publisher's Note
Springer Nature remains neutral with regard to jurisdictional claims in published maps and institutional affiliations.

References

Babapoor A, Karimi G, Khorram M (2016) Fabrication and characterization of nanofiber-nanoparticle-composites with phase change materials by electrospinning. Appl Therm Eng 99:1225–1235. https://doi.org/10.1016/j.applthermaleng.2016.02.026

Cai Y, Sun G, Liu M, Zhang J, Wang Q, Wei Q (2015) Fabrication and characterization of capric–lauric–palmitic acid/electrospun SiO$_2$ nanofibers composite as form-stable phase change material for thermal energy storage/retrieval. Sol Energy 118:87–95. https://doi.org/10.1016/j.solener.2015.04.042

Chen C, Liu W, Wang Z, Peng K, Pan W, Xie Q (2015) Novel form stable phase change materials based on the composites of polyethylene glycol/polymeric solid-solid phase change material. Sol Energy Mater Sol Cells 134:80–88. https://doi.org/10.1016/j.solmat.2014.11.039

Collinson SR, Thielemans W (2010) The catalytic oxidation of biomass to new materials focusing on starch, cellulose and lignin. Coord Chem Rev 254(15–16):1854–1870. https://doi.org/10.1016/j.ccr.2010.04.007

Fang G, Li H, Chen Z, Liu X (2010) Preparation and characterization of flame retardant *n*-hexadecane/silicon dioxide composites as thermal energy storage materials. J Hazard Mater 181(1–3):1004–1009. https://doi.org/10.1016/j.jhazmat.2010.05.114

Feng L, Zheng J, Yang H, Guo Y, Li W, Li X (2011) Preparation and characterization of polyethylene glycol/active carbon composites as shape-stabilized phase change materials. Sol Energy Mater Sol Cells 95(2):644–650. https://doi.org/10.1016/j.solmat.2010.09.033

He L, Li J, Zhou C, Zhu H, Cao X, Tang B (2014) Phase change characteristics of shape-stabilized PEG/SiO2 composites using calcium chloride-assisted and temperature-assisted sol gel methods. Sol Energy 103:448–455. https://doi.org/10.1016/j.solener.2014.02.042

Huang Z, Gao X, Xu T, Fang Y, Zhang Z (2014) Thermal property measurement and heat storage analysis of LiNO$_3$/KCl—expanded graphite composite phase change material. Appl Energy 115:265–271. https://doi.org/10.1016/j.apenergy.2013.11.019

Khodadadi JM, Fan L, Babaei H (2013) Thermal conductivity enhancement of nanostructure-based colloidal suspensions utilized as phase change materials for thermal energy storage: a review. Renew Sustain Energy Rev 24:418–444. https://doi.org/10.1016/j.rser.2013.03.031

Lafdi K, Mesalhy O, Elgafy A (2008) Graphite foams infiltrated with phase change materials as alternative materials for space and terrestrial thermal energy storage applications. Carbon 46(1):159–168. https://doi.org/10.1016/j.carbon.2007.11.003

Li H, Lei Z, Liu C, Zhang Z, Lu B (2014) Photocatalytic degradation of lignin on synthesized Ag-AgCl/ZnO nanorods under solar light and preliminary trials for methane fermentation. Bioresour Technol 175C:494–501. https://doi.org/10.1016/j.biortech.2014.10.143

Luo H, Ning XA, Liang X, Feng Y, Liu J (2013) Effects of sawdust-CPAM on textile dyeing sludge dewaterability and filter cake properties. Bioresour Technol 139:330–336. https://doi.org/10.1016/j.biortech.2013.04.035

Mateo S, Gonzalez del Campo A, Canizares P, Lobato J, Rodrigo MA, Fernandez FJ (2014) Bioelectricity generation in a self-sustainable microbial

Yang *et al. Bioresour. Bioprocess.* (2017) 4:52

Page 12 of 12

solar cell. Bioresour Technol 159:451–454. https://doi.org/10.1016/j.biortech.2014.03.059

Memon SA (2014) Phase change materials integrated in building walls: a state of the art review. Renew Sustain Energy Rev 31:870–906. https://doi.org/10.1016/j.rser.2013.12.042

Qian Y, Wei P, Jiang P, Li Z, Yan Y, Liu J (2013) Preparation of a novel PEG composite with halogen-free flame retardant supporting matrix for thermal energy storage application. Appl Energy 106:321–327. https://doi.org/10.1016/j.apenergy.2012.12.070

Qian T, Li J, Ma H, Yang J (2015a) The preparation of a green shape-stabilized composite phase change material of polyethylene glycol/SiO$_2$ with enhanced thermal performance based on oil shale ash via temperature-assisted sol–gel method. Sol Energy Mater Sol Cells 132:29–39. https://doi.org/10.1016/j.solmat.2014.08.017

Qian T, Li J, Min X, Deng Y, Guan W, Ma H (2015b) Polyethylene glycol/mesoporous calcium silicate shape-stabilized composite phase change material: preparation, characterization, and adjustable thermal property. Energy 82:333–340. https://doi.org/10.1016/j.energy.2015.01.043

Sarı A (2015) Fabrication and thermal characterization of kaolin-based composite phase change materials for latent heat storage in buildings. Energy Build 96:193–200. https://doi.org/10.1016/j.enbuild.2015.03.022

Sarı A, Karaipekli A (2007) Thermal conductivity and latent heat thermal energy storage characteristics of paraffin/expanded graphite composite as phase change material. Appl Therm Eng 27(8–9):1271–1277. https://doi.org/10.1016/j.applthermaleng.2006.11.004

Shin HK, Park M, Kim H-Y, Park S-J (2015) Thermal property and latent heat energy storage behavior of sodium acetate trihydrate composites containing expanded graphite and carboxymethyl cellulose for phase change materials. Appl Therm Eng 75:978–983. https://doi.org/10.1016/j.applthermaleng.2014.10.035

Shukla A, Zhang Y-H, Dubey P, Margrave JL, Shukla SS (2002) The role of sawdust in the removal of unwanted materials from water. J Hazard Mater 95(1):137–152

Sobolciak P, Karkri M, Al-Maadeed MA, Krupa I (2016) Thermal characterization of phase change materials based on linear low-density polyethylene, paraffin wax and expanded graphite. Renew Energy 88:372–382. https://doi.org/10.1016/j.renene.2015.11.056

Tang F, Su D, Tang Y, Fang G (2015) Synthesis and thermal properties of fatty acid eutectics and diatomite composites as shape-stabilized phase change materials with enhanced thermal conductivity. Sol Energy Mater Sol Cells 141:218–224. https://doi.org/10.1016/j.solmat.2015.05.045

Tang B, Wang L, Xu Y, Xiu J, Zhang S (2016) Hexadecanol/phase change polyurethane composite as form-stable phase change material for

thermal energy storage. Sol Energy Mater Sol Cells 144:1–6. https://doi.org/10.1016/j.solmat.2015.08.012

Tian H, Wang W, Ding J, Wei X, Song M, Yang J (2015) Thermal conductivities and characteristics of ternary eutectic chloride/expanded graphite thermal energy storage composites. Appl Energy 148:87–92. https://doi.org/10.1016/j.apenergy.2015.03.020

Wang S, Qin P, Fang X, Zhang Z, Wang S, Liu X (2014) A novel sebacic acid/expanded graphite composite phase change material for solar thermal medium-temperature applications. Sol Energy 99:283–290. https://doi.org/10.1016/j.solener.2013.11.018

Wang Y, Liang D, Liu F, Zhang W, Di X, Wang C (2017) A polyethylene glycol/hydroxyapatite composite phase change material for thermal energy storage. Appl Therm Eng 113:1475–1482. https://doi.org/10.1016/j.applthermaleng.2016.11.159

Xu B, Li Z (2014) Paraffin/diatomite/multi-wall carbon nanotubes composite phase change material tailor-made for thermal energy storage cement-based composites. Energy 72:371–380. https://doi.org/10.1016/j.energy.2014.05.049

Zeng J-L, Zhu F-R, Yu S-B, Xiao Z-L, Yan W-P, Zheng S-H, Zhang L, Sun L-X, Cao Z (2013) Myristic acid/polyaniline composites as form stable phase change materials for thermal energy storage. Sol Energy Mater Sol Cells 114:136–140. https://doi.org/10.1016/j.solmat.2013.03.006

Zhang Z, Zhang N, Peng J, Fang X, Gao X, Fang Y (2012) Preparation and thermal energy storage properties of paraffin/expanded graphite composite phase change material. Appl Energy 91(1):426–431. https://doi.org/10.1016/j.apenergy.2011.10.014

Zhang Z, Shi G, Wang S, Fang X, Liu X (2013) Thermal energy storage cement mortar containing *n*-octadecane/expanded graphite composite phase change material. Renew Energy 50:670–675. https://doi.org/10.1016/j.renene.2012.08.024

Zhao J, Guo Y, Feng F, Tong Q, Qv W, Wang H (2011) Microstructure and thermal properties of a paraffin/expanded graphite phase-change composite for thermal storage. Renew Energy 36(5):1339–1342. https://doi.org/10.1016/j.renene.2010.11.028

Zhenyu S, Zhanqiang L, Hao S, Xianzhi Z (2016) Prediction of contact angle for hydrophobic surface fabricated with micro-machining based on minimum Gibbs free energy. Appl Surf Sci 364:597–603. https://doi.org/10.1016/j.apsusc.2015.12.199

Zhong Y, Li S, Wei X, Liu Z, Guo Q, Shi J, Liu L (2010) Heat transfer enhancement of paraffin wax using compressed expanded natural graphite for thermal energy storage. Carbon 48(1):300–304. https://doi.org/10.1016/j.carbon.2009.09.033